



Peroxo–tungstate(VI) complexes: syntheses, characterization, reactivity, and DFT studies

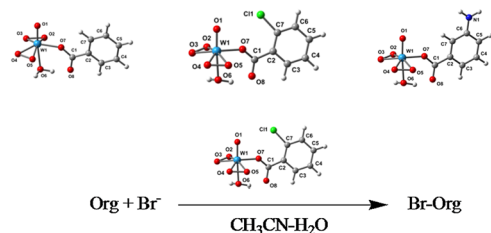
Nandita Das¹ · Shubhamoy Chowdhury² · Ranendra N. Dutta Purkayastha¹

Received: 12 October 2018 / Accepted: 20 April 2019
© Springer-Verlag GmbH Austria, part of Springer Nature 2019

Abstract

Three new oxodiperoxo–tungsten(VI) complexes containing benzene core carboxylic acids, viz., benzoic acid, 2-chlorobenzoic acid, and 3-aminobenzoic acid as co-ligands have been synthesized from reaction of $\text{Na}_2\text{WO}_6\text{H}_4$, 30% H_2O_2 and the corresponding co-ligands in aqueous medium. The compounds have been comprehensively characterized by elemental analyses, FT-IR, ^1H NMR, UV–Vis spectral studies as well as by mass spectrometric and TGA analyses. The infrared spectra suggest occurrence of terminally bonded $\text{W}=\text{O}$ as well as triangular bidentate peroxo groups (C_{2v}) and monodentate carboxylate group bound to the WO^{4+} center. The mass spectra of the compounds are in good agreement with proposed molecular formulations. Thermogravimetric analyses indicate the existence of both lattice and coordinated water molecules in the complexes. Density functional theory (DFT) calculations were used to compute the frequencies of relevant vibrational modes, electronic properties and also to investigate structure of the compounds. Compound potassium(aquo)(2-chlorobenzoato)oxodiperoxo–tungstate(VI)dihydrate acts as an oxidant for bromide ion in aqueous phase bromination of chosen organic substrates to their corresponding bromo-organics.

Graphical abstract



Keywords Bromination · Density functional theory · Peroxo–tungsten complexes · Spectroscopy

Electronic supplementary material The online version of this article (<https://doi.org/10.1007/s00706-019-02435-1>) contains supplementary material, which is available to authorized users.

✉ Ranendra N. Dutta Purkayastha
rndp09@gmail.com

- 1 Department of Chemistry, Tripura University, Suryamaninagar, Tripura 799022, India
- 2 Department of Chemistry, University of Gour Banga, Malda, West Bengal 732103, India

Introduction

Hydrogen peroxide readily combines with transition metals such as V(V), Mo(VI), Nb(V), and W(VI) forming a number of peroxo complexes whose nature depends on the pH as well as relative concentration of the reagents [1]. Peroxo complexes of transition metals, viz., V, Mo, Nb and W have attracted considerable attention because of their intrinsic importance in biological chemistry, structural chemistry, material science, and catalytic activity [2–8]. The chemistry of peroxo–tungsten complexes has been an area of significant interest for a number of reasons including their role as stoichiometric and effective catalytic

oxidants and oxo-transfer agents in host of organic transformations [9–14]. Some of the peroxo–tungsten species have been recognized as potential insulin mimics and recently shown to possess superior bromoperoxidase activity compared to that of peroxo–vanadates [15–17]. As emphasized, the peroxo–tungsten complexes are efficient and relatively selective oxidants for many organic and inorganic species and at the same time less polluting; thus, they may provide a valuable eco-friendly alternative [18, 19].

In continuation of our interest in peroxo–tungsten chemistry [20], we have endeavored to synthesize and explore some properties of new oxodiperoxo–tungstate(VI) complexes incorporating benzene-core carboxylic acids as hetero-ligands. As part of exploration of transition metal compound-catalyzed aqueous medium organic transformations [21], we were particularly interested to ascertain whether the synthesized peroxo–tungstate(VI) complexes could act as oxidant for halide (bromide) with good activity at neutral pH in aqueous medium. The important role of halogenated compounds in chemistry combined with poor economic and environmental efficiency of the common halogenating systems makes catalytic halo-peroxidation an attractive alternative and important aspect in modern catalysis [22]. The inspiration for catalytic halo-peroxidation also comes from biological systems in which enzymes, such as haloperoxidase (HPS) are able to activate hydrogen peroxide or oxygen. In these systems, the oxidation of halogen brings further the corresponding oxidized electrophilic counterpart which is able to halogenate organic substrates [21]. Thus, this bio-mimetic approach can be utilized as an alternative route to traditional bromination reaction. Among the halogenating processes, bromination of organic substrates particularly aromatics has generated significant interest in recent years due to the commercial importance of such compounds as potent anti-tumor, antibacterial, anti-fungal, anti-neoplastic, antiviral, and anti-oxidizing agents [23–25]; however, the hazards associated with traditional bromination are serious and cannot be overlooked [26].

Herein, we report synthesis, physico-chemical characterization of mononuclear oxodiperoxo–tungstate(VI), containing benzene-core carboxylic acids, viz., benzoic acid, 2-chlorobenzoic acid, 3-aminobenzoic acid as the hetero-ligands and assessment of their activity in oxidative bromination of organic substrates. Additionally, density functional theory (DFT) calculations were used to study and classify the structures and to simulate the infrared absorption frequencies and electronic absorption bands. The comparison between the theoretical and the experimental values for infrared, electronic absorption frequencies in principle provide an excellent means for structure elucidation.

Results and discussion

The reaction of hydrogen peroxide with WO_4^{4-} leading to a complex peroxo–tungstate(VI) of definite composition is highly dependent on the pH of the reaction medium (vide infra). The evaluation of an appropriate pH for successful synthesis of peroxo–metal species is emphasized to be an important pre-requisite [27–30]. In our endeavor to synthesize mononuclear hetero-ligand oxodiperoxo–tungstate(VI), reaction of Na_2WO_6 with 30% H_2O_2 and the corresponding hetero-ligands in aqueous medium was strategically carried out in weakly alkaline solution. The suitable pH for coordination of both peroxide and the hetero-ligands was ascertained to be ca. 7–7.5, which favored the formation of mononuclear oxodiperoxo species of tungsten(VI) in solution. Compounds were isolated as microcrystalline solid of their potassium salt. The pH of ca. 7–7.5 of the reaction medium was maintained by the addition of 2 N KOH solution which also served as the source of counter-cation for the anionic complexes. The other factors such as the sequence of addition of the reactants, maintenance of reaction time and reaction temperature (0–4 °C) were also equally important for successful synthesis of the desired compounds. In all these cases of syntheses of oxodiperoxo–tungstate(VI) complexes, addition of pre-cooled acetone facilitated precipitation and afforded the compounds in high yields. The synthesized compounds **1–3** are diamagnetic as evidenced from the magnetic susceptibility measurements in conformity with the presence of hexavalent tungsten in each case.

Characterization and assessment of structure

The synthesized hetero-ligand potassium(aquo)oxodiperoxo–tungstate(VI) (**1–3**) is a white microcrystalline solid and soluble in water. Solubility of the compounds in water made them suitable to be used as catalytic oxidants in aqueous phase bromination of organic substrates. Due to increasing environmental concern, the aqueous medium organic transformations have currently gained significant importance [31, 32]. All the synthesized compounds decompose in dilute sulfuric acid solution liberating hydrogen peroxide quantitatively, thus facilitating the determination of active oxygen contents of the compounds. Chemical determination of the active oxygen, which was considered to be very crucial to ascertain the number of peroxide (O_2^{2-}) group coordinated to WO_4^{4-} center, was accomplished by redox titration involving a standard Ce^{4+} solution and also separately with standard KMnO_4 solution. The estimation was carried out in the presence of boric acid to prevent any loss of active oxygen.

The results of elemental analyses suggest the occurrence of two O_2^{2-} groups per WO^{4+} center and C, H, N analyses indicate W:hetero-ligand ratio as 1:1 in accordance with the formulation (1–3). Molar conductance of the complexes in aqueous solution (10^{-3} M) exhibits values of $130 \Omega^{-1} \text{ mol}^{-1} \text{ cm}^{-1}$ as expected for a uni-univalent electrolyte. Despite several attempts, it was not possible to obtain suitable crystals of the compounds for single-crystal X-ray diffraction.

Infrared spectra

The infrared spectra of the complexes revealed sufficiently that well-resolved spectral pattern (Figs. S1–S3, supplementary information) involves absorptions due to $\text{W}=\text{O}$ stretching, coordinated peroxide, hetero-ligands, viz., benzoate, 2-chlorobenzoate, 3-aminobenzoate and water molecules. The strong and sharp band at ca. $907\text{--}917 \text{ cm}^{-1}$ in the spectra of the complexes is consistent with the presence of a terminally bonded $\text{W}=\text{O}$ group in each case [33]. A triangularly bonded peroxide (C_{2v}) exhibits characteristic infrared absorptions with $\nu(\text{O}-\text{O})$ at ca. $830\text{--}870 \text{ cm}^{-1}$ and ν_2 , ν_3 which involve symmetric and asymmetric metal–oxygen stretching ($\text{M}-\text{O}_2$) in the region $500\text{--}700 \text{ cm}^{-1}$ [34, 35]. In spectra of complexes 1, 2, and 3, occurrence of a strong and sharp band at ca. $829\text{--}838 \text{ cm}^{-1}$ ascribed to $\nu(\text{O}-\text{O})$ vibration and suggests that the peroxide group (O_2^{2-}) is bonded to the WO^{4+} center in a triangular bidentate (C_{2v}) fashion [34, 35]. Medium- to weak-intensity bands in the regions $565, 694 \text{ cm}^{-1}$ for 1; $547, 702 \text{ cm}^{-1}$ for 2; and $565, 734 \text{ cm}^{-1}$ in case of 3 are assigned to symmetric and asymmetric stretching vibrations, respectively, of the WO_2 triangle formed from terminally η^2 -coordinated O_2^{2-} ligand [36–39]. Absorption assignable to asymmetric stretching of coordinated carboxylate moiety of the hetero-ligands benzoate, 2-chlorobenzoate and 3-aminobenzoate appeared at ca. $1606\text{--}1640 \text{ cm}^{-1}$ whereas the corresponding symmetric vibrations were observed in the region $1431\text{--}1470 \text{ cm}^{-1}$. The observed difference in frequency between asymmetric and symmetric stretching vibrations of carboxylate group, $\Delta\nu$ ($\nu_{\text{assy}} - \nu_{\text{sym}} = \Delta\nu$) greater than 200 cm^{-1} is characteristic of monodentate coordination of carboxylate group [40, 41]. The presence of water molecules in each of the complexes 1–3 as evidenced in thermogravimetric analyses was also inferred from the presence of strong absorption in the range of $3400\text{--}3500 \text{ cm}^{-1}$ due to the $\nu(\text{O}-\text{H})$ vibration. However, the corresponding bending mode of water $\delta(\text{H}-\text{O}-\text{H})$ could not be ascertained with certainty as it occurred in the CO_2 stretching frequency region. The slight broadening of $\nu(\text{O}-\text{H})$ band related to water suggests a clear possibility of intramolecular hydrogen bonding by the participation of tungsten oxygen. For compound 3 containing 3-aminobenzoate as hetero-ligand, $\nu(\text{N}-\text{H})$ could not be assigned with

certainty owing to its overlapping with $\nu(\text{O}-\text{H})$ mode of water resulting in a broad band at ca. $3368\text{--}3500 \text{ cm}^{-1}$. The results of IR spectral analyses are in close agreement with the proposed molecular structures of the complexes under consideration.

Mass spectra

The mass spectra of the compounds were recorded to ascertain the molecular mass of the compounds and are presented in Figs. S8–S10. The mass spectra of the complexes show an extensive fragmentation pattern and most of the fragment ions occur in a group of peaks due to tungsten isotopes. Appearances of peaks beyond the molecular ion peak for each of complexes 1–3 suggest association of the complexes in gaseous state. In ESI spectrum of compound 1, the peak at $m/z = 478.79$ is due to the molecular ion peak (calc. 478.09). Observance of peak at $m/z = 426.13$ (calc. 426.05) and at $m/z = 235.21$ (calc. 235.85) is assignable to fragments ($\text{KWO}_7\text{C}_7\text{H}_5 + 2\text{H}^+$) and ($\text{WO}_3 + 4\text{H}^+$), respectively. For compound 2, molecular ion peak with appreciable intensity was observed at $m/z = 494.76$ (calc. 494.52). Compound 2 also shows peaks at $m/z = 478.79$ (calc. 478.52), 394.85 (calc. 394.49), and 358.81 (calc. 358.39) assigned to ($\text{KWO}_8\text{C}_7\text{H}_6\text{Cl} + 2\text{H}^+$), ($\text{KWO}_3\text{C}_7\text{H}_4\text{Cl}$), and ($\text{WO}_3\text{C}_7\text{H}_4\text{Cl} + 3\text{H}^+$), respectively. In the mass spectrum of compound 3, a prominent peak at $m/z = 494.75$ (calc. 494.10) is attributable to $[\text{M} + \text{H}]^+$. Appearance of peaks at $m/z = 478.78$ (calc. 478.09) and at 410.80 (calc. 410.06) is reasonable to assign to fragments ($\text{KWO}_9\text{C}_7\text{H}_{10}\text{N} + 3\text{H}^+$) and ($\text{KWO}_5\text{C}_7\text{H}_6\text{N} + 3\text{H}^+$), respectively. Due to extensive fragmentation and association of fragment ions in each compound, all the observed peaks could not be assigned. Overall, the mass spectral data are in good agreement with the composition and expected structures of the complexes proposed on the basis of elemental analyses and spectral data.

Thermogravimetric analysis (TGA)

Thermogravimetric analysis data indicate that after the initial dehydration, the compounds undergo gradual decomposition on heating up to a temperature of $900 \text{ }^\circ\text{C}$ (Figs. S11–S13). Interestingly, the compounds do not explode on heating, although many peroxo–metal compounds have been known to decompose explosively on heating [42]. The thermograms of the compounds showed that the first-stage decomposition occurs in the temperature range of $120\text{--}130 \text{ }^\circ\text{C}$ with the loss of molecules of lattice water from the complexes. The corresponding weight losses of 7.49%, 7.10%, and 7.16% for complexes 1, 2, and 3 are in good agreement with the values of 7.53%, 7.03%, and 7.30% calculated for two molecules of water of crystallization. A slightly higher temperature is required for the removal of

lattice water probably due to the existence of intra-molecular hydrogen bonding in the complexes. The next decomposition stage in the temperature range of 180–190 °C with the corresponding weight loss of 4.12% (calc. 4.07%), 3.88% (calc. 3.78%) 4.08% (calc. 3.93%), respectively, is attributable to loss of coordinated water molecule from the complexes. A further increase in temperature leads to continuous degradation due to loss of peroxy groups as well as fragmentation of hetero-ligands up to a final temperature of 900 °C. The solid residue remaining after complete degradation is attributed to the formation oxo–tungsten species. Thermogravimetric data of the compounds show that the synthesized complexes have relatively good thermal stability and provide further evidence in support of the composition and formula assigned to the compounds.

¹H NMR study

The ¹H NMR spectra for the complexes **1**, **2**, and **3** in D₂O are presented in Figs. S14–S16, respectively, and corresponding chemical shift values for the complexes and the free benzene core carboxylic acids are presented in Table 1. A close similarity was observed in the ¹H NMR spectra of the complexes and the spectra of the respective carboxylic acid displaying well-resolved resonances with expected integration and peak multiplicities. The spectra of the complexes **1** and **2** containing benzoate and 2-chlorobenzoate showed distinct upfield shift of the proton signals (C-2, C-3, C-4, C-5, C-6) relative to the free ligand. The significant coordination-induced shift $\Delta\delta$ ($\delta_{\text{free carboxylic acid}} - \delta_{\text{complex}}$) occurred as expected, suggesting appreciable metal–ligand coordination [43, 44]. However, in case of compound **3** containing 3-aminobenzoate as the co-ligand, the proton signals

attached to carbon atom (C-2, C-4, C-5, and C-6) showed distinct downfield shift relative to the free co-ligand. The observed downfield shift may be due to conjugation of lone pair of electrons in nitrogen with ring π -electrons. The signals of protons attached to nitrogen of –NH₂ group could not be observed probably due to exchange with the solvent D₂O.

Thus, ¹H NMR spectra testify the presence of the complex species in solution, suggesting that the compounds did not hydrolyze and retained their identity in solution. Thus, apart from valuable structural information, the NMR data also provided evidence in support of the stability of the compounds in solution for reasonable period of time as observed in the solution state electronic spectra of the complexes (vide infra).

Substrate bromination in aqueous–organic medium

As emphasized (vide infra), the importance of halogenated compounds and increasing awareness about environmental safety and catalytic halo-peroxidaion has gained significant importance as an alternative route to that of classical halogenation of organic substrates. It is reported in the literature that transition metal–peroxy compounds can oxidize bromide leading to the formation of an active bromination-competent species (“Br⁺ equivalent”, e.g., HOBr, Br₂, Br₃[−]) in situ which mediates the bromination of organic substrates to afford bromo-organics [21].

It has been observed that stoichiometry of the reaction requires for one equivalent of substrate, one equivalent of oxidant, i.e., compound **2** and two equivalents of halide (KBr) is optimal. The solvent mixture of C₂H₃N:H₂O (1:1, 8 cm³) gave a reasonably good yield of the brominated products. The notable feature of the methodology is that no extra addition of acid was required for stoichiometric bromination reaction of the substrates. The reactions were conducted in water–acetonitrile medium because of environmental safety consideration, although similar reactions are possible in dichloromethane as well. The substrate for aqueous phase bromination included activated aromatics such as 1-naphthol, 2-naphthol, salicylaldehyde, acetanilide, vanillin and hetero-aromatics, viz., imidazole and 2-methylimidazole. Compound **2** satisfactorily catalyzed the oxidative bromination of the activated aromatics to their corresponding brominated products in moderately good yield (Table 2). The bromination of hetero-aromatics such as imidazole and 2-methylimidazole was carried out using higher proportion of KBr (substrate:KBr 1:3) to afford the respective bromo derivatives. A 1:2 stoichiometry of substrate to KBr did not produce the desired result. A blank reaction, i.e. similar reaction without the addition of compound **2**, did not afford the brominated products. Preferential bromination at either *ortho* or *para* position of the aromatic ring suggests an electrophilic mechanism.

Table 1 ¹H (δ /ppm) of **1**, **2**, and **3** in D₂O as the solvent (25 °C)

| | Free ligand | Compound |
|--|-------------|----------|
| KWO ₁₀ C ₇ H ₁₁ (1) | | |
| C-2, C-6 | 8.18 | 7.72 |
| C-3, C-5 | 7.47 | 7.32 |
| C-4 | 7.60 | 7.39 |
| KWO ₁₀ C ₇ H ₁₀ Cl (2) | | |
| C-3 | 8.48 | 7.14 |
| C-4 | 7.51 | 7.18 |
| C-5 | 7.34 | 7.06 |
| C-6 | 8.03 | 7.23 |
| KWO ₁₀ C ₇ H ₁₂ N (3) | | |
| C-2 | 7.33 | 8.24 |
| N–H | 4 | – |
| C-4 | 6.80 | 7.5 |
| C-5 | 7.22 | 8.10 |
| C-6 | 7.49 | 8.5 |

Table 2 Bromination of aromatic substrates mediated by compound **2**

| Substrate | Product | Yield/% |
|-------------------|--|----------------|
| 1-Naphthol | 2,4-Dibromo-1-naphthol | 65 |
| 2-Naphthol | 1-Bromo-2-naphthol | 89 |
| Salicylaldehyde | 5-Bromosalicylaldehyde (a) 3,5-Dibromosalicylaldehyde (b) | 52 (a), 18 (b) |
| Acetanilide | 4-Bromoacetanilide | 69 |
| Vanillin | 5-Bromovanilline | 81 |
| Imidazole | 4-Bromoimidazole(a) 4,5-Dibromoimidazole(b) | 16 (a), 27 (b) |
| 2-Methylimidazole | 4-Bromo-2-methylimidazole (a) 4,5-Dibromo-2-methylimidazole (b) | 26 (a), 71 (b) |

In summary, we have shown that bromination of organic substrates can be achieved by carrying out reaction of organic substrates including heterocyclic compounds, with potassium bromide and compound **2**. The methodology provides an efficient, straightforward and benign alternative to rather hazardous classical bromination protocols, opening an opportunity to gain easy access to a variety of bromo organics.

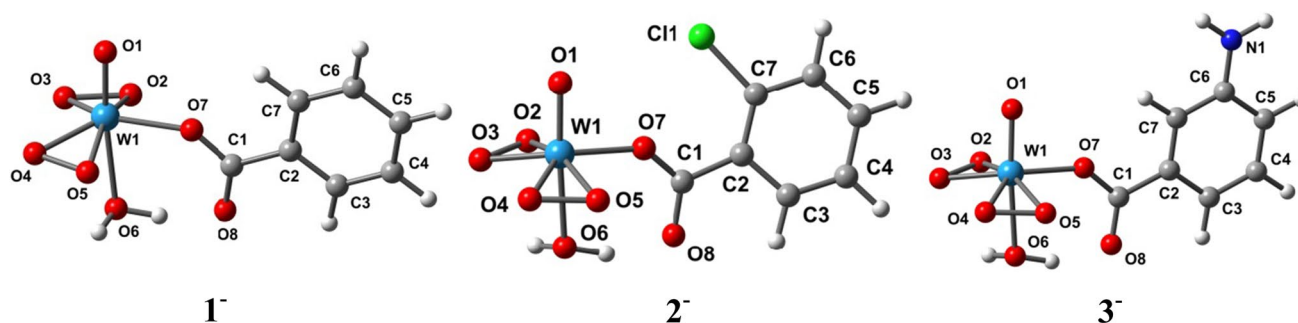
Theoretical investigation

The optimized structures of compounds **1**[−], **2**[−], and **3**[−] are shown in Fig. 1, and Table S1 represents the calculated bond distances and bond angles. The W=O bond lengths for the optimized structures **1**[−], **2**[−], and **3**[−] are found to be 1.749 Å, 1.730 Å, and 1.733 Å, respectively, which are in the typical range of distance (~1.620 to ~1.785 Å) reported for oxo–tungstate complexes [45–47]. The O–O (per bond) bond lengths of 1.555 Å (on an average) of the coordinated peroxy groups for the optimized structures of **1**[−], **2**[−], and **3**[−] are in the range usually observed for the peroxy–metal complexes [1, 48]. The W–O (peroxy oxygen) bond length for the species **1**[−], **2**[−], and **3**[−] were observed at ca. 1.974–1.995 Å similar to that of the

reported oxo–tungstate complexes [1, 46–48]. A good agreement exists among the calculated geometry of the model structures of **1**[−], **2**[−], and **3**[−] and the experimental as well as the calculated structure geometry of the reported ones [1, 45–50].

IR spectra

Both the diagnostic experimental and calculated (non-scaled) IR frequencies of the species **1**[−], **2**[−], and **3**[−] are shown in Fig. 2 and their assignments are presented in Table 3. The characteristic feature of IR spectrum of free carboxylic group is occurrence of a band in the region 1700–1800 cm^{−1} due to C=O stretching vibration. In solid state, most of the carboxylic acids usually form a dimeric structure due to the existence of hydrogen bonding between the –CO₂H groups. In such cases, two $\nu(\text{C}=\text{O})$ vibrations are expected, one is Raman active (symmetric stretching) while the other IR active (anti-symmetric stretching) [51]. The anti-symmetric stretching vibration of carboxylate group for complexes **1**[−], **2**[−], and **3**[−] are observed at ca. 1640, 1640, and 1606 cm^{−1}, respectively. The observed anti-symmetric carboxylate stretching bands are at a lower frequency than the free carboxylic group which is theoretically reproduced at ca. 1641–1653 cm^{−1}. The observed shifts in the carboxylic frequencies are expected as the coordination of CO₂[−] moiety to the metal center generally results in a decrease of carboxylate stretching frequency. The IR spectra of **1**[−], **2**[−], and **3**[−] also exhibit characteristic vibrations due to W=O moiety at 914, 907, and 914 cm^{−1} which are theoretically reproduced at 933.96, 981.14, and 974.83 cm^{−1}, the range expected for such vibration [33, 52, 53]. The maximum deviations of the calculated IR frequencies for complex ions **1**[−], **2**[−], and **3**[−] from their respective experimental values are less than 8%. These variations are quite reasonable, as the theoretical calculations are based on the gas phase and only anionic species of the respective molecules were considered. The computed data are often at variance with the experimentally obtained data [54].

**Fig. 1** Geometry optimized structures of **1**[−], **2**[−], and **3**[−]

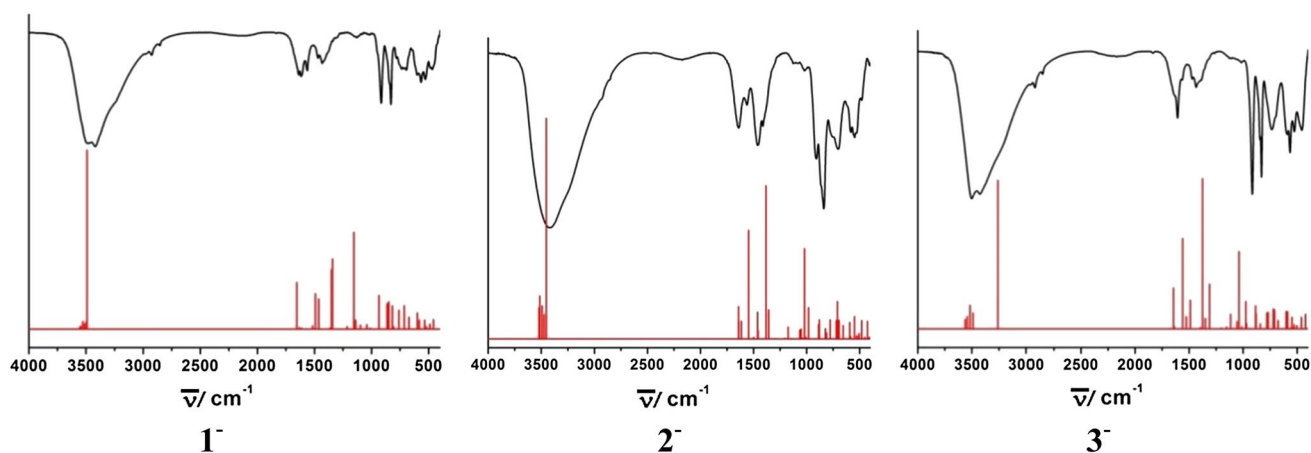


Fig. 2 The experimental (black) and calculated (red) vibrational transitions of **1⁻**, **2⁻**, and **3⁻**

Table 3 The diagnostic experimental and calculated IR frequencies for **1⁻**, **2⁻**, and **3⁻**

| Compounds | Experimental/cm ⁻¹ | Theoretical/cm ⁻¹ | Assignments |
|--|-------------------------------|------------------------------------|--|
| KWO ₁₀ C ₇ H ₁₁ (1) | 3486br | 3512.04, 3528.36, 3545.78, 3555.60 | ν(C-H ^{Ar}) |
| | 3419br | 3490.20 | ν(O-H) |
| | 1640 | 1653.89 | ν _{asy} (CO ₂ ⁻) |
| | 1431 | 1461.26 | ν _{sym} (CO ₂ ⁻) |
| | 914 | 933.96 | ν(W=O) |
| | 829 | 852.33 | ν(O-O) |
| | 694 | 713.36 | ν _{asy} (W-O ₂) |
| | 565 | 582.48 | ν _{sym} (W-O ₂) |
| KWO ₁₀ C ₇ H ₁₀ Cl (2) | 3265br, 3421 br | 3453.84, 3472.45, 3493.17, 3513.55 | ν(O-H), ν(C-H ^{Ar}) |
| | 907 | 981.14 | ν(W=O) |
| | 838 | 879.58, 886.38 | ν(O-O) |
| | 696 | 709.63 | ν _{asy} (W-O ₂) |
| | 547 | 549.64 | ν _{sym} (W-O ₂) |
| | 1640 | 1641.29 | ν _{asy} (CO ₂ ⁻) |
| | 1459 | 1462.34 | ν _{sym} (CO ₂ ⁻) |
| KWO ₁₀ C ₇ H ₁₂ N(3) | 3502 br | 3489.22, 3517.75, 3543.06, 3561.34 | ν(C-H ^{Ar}), ν(N-H) |
| | 3424 br | 3259.67 | ν(O-H) |
| | 914 | 974.83 | ν(W=O) |
| | 829 | 885.37, 879.37 | ν(O-O) |
| | 734 | 719.55 | ν _{asy} (W-O ₂) |
| | 565 | 589.57 | ν _{sym} (W-O ₂) |
| | 1606 | 1643.84 | ν _{asy} (CO ₂ ⁻) |
| | 1434 | 1487.74 | ν _{sym} (CO ₂ ⁻) |

Molecular orbital description and electronic spectra

Close analogy was observed among the observed UV-Vis spectral pattern of the complexes recorded in aqueous solution (10⁻³ M). The spectra exhibited a medium-intensity band at ca. 254–264 nm (Figs. S4–S6) [$\epsilon_M = 0.45 \times 10^3 \text{ dm}^3 \text{ mol}^{-1} \text{ cm}^{-1}$ (**1**), $0.026 \times 10^3 \text{ dm}^3 \text{ mol}^{-1} \text{ cm}^{-1}$ (**2**), $0.18 \times 10^3 \text{ dm}^3 \text{ mol}^{-1} \text{ cm}^{-1}$ (**3**)] assignable to transition from peroxo group to tungsten charge transfer

(LMCT) band [55]. The observed high-energy band at ca. 200–205 nm [$\epsilon_M = 3.7 \times 10^3 \text{ dm}^3 \text{ mol}^{-1} \text{ cm}^{-1}$ (**1**), $0.49 \times 10^3 \text{ dm}^3 \text{ mol}^{-1} \text{ cm}^{-1}$ (**2**), $3.3 \times 10^3 \text{ dm}^3 \text{ mol}^{-1} \text{ cm}^{-1}$ (**3**)] may be assigned to intra-ligand charge transfer transition [55], also reproduced in theoretical calculation. There is no evidence of a d-d transition consistent with the presence of W(VI). The intensity of the absorption band remains unaltered (0–3 h) (Fig. S7); however, it gradually

decreases with time (> 3 h) indicating partial loss of peroxide in solution on standing for prolonged period.

The absorption spectra of 1^- , 2^- , and 3^- as discussed are simulated in the presence of the solvent model (aqueous) employing the TD–DFT methods with the identical basis set and functional as used in geometry optimization and frequency calculations. The resultant simulated data are in good agreement with the experimentally obtained data (Fig. 3).

The calculated spin-allowed singlet–singlet electronic transitions and the experimentally obtained data for 1^- , 2^- , and 3^- in aqueous solution are summarized in Table 4. The selected transitions of 1^- , 2^- , and 3^- having significant oscillator strengths are incorporated and screened. The transitions only with orbital contributions larger than 5% are taken into account for molecular ions under consideration.

A schematic representation of the energy of MOs and contours of the selected HOMO and LUMO orbitals of 1^- , 2^- , and 3^- is presented in Figs. 4 and 5. The energy gap between HOMO and LUMO for 1^- , 2^- , and 3^- is found to be 2.981, 5.032, and 3.800 eV, respectively. In solution, the highest occupied molecular orbitals (HOMOs) of 1^- and 2^- have major contribution from peroxo group whereas in case of 3^- , the major contribution is received from ligand 3-aminobenzoate. The unoccupied orbitals L + 2, L + 3 for 1^- , L + 1, L + 2 for 2^- , and L, L + 2 for 3^- exhibit considerable amount of metallic character. The energy of transitions in solution was calculated at 267.97, 241.26, and 345.01 nm for compounds 1^- , 2^- , and 3^- , respectively. In solution, the calculated absorption bands at 267.97, 241.26, and 345.01 nm for 1^- , 2^- , and 3^- are assigned to (H-1 \rightarrow L, H-1 \rightarrow L + 2, H \rightarrow L + 3), (H-1 \rightarrow L + 2, H-4 \rightarrow L + 1, H-3 \rightarrow L, H-3 \rightarrow L + 1), and (H-1 \rightarrow L, H \rightarrow L + 1, H \rightarrow L + 2) modes of transitions, respectively. MO analyses of these transitions show that a significant amount of electron density is transferred from the hetero-ligand that is benzene-core carboxylic

acid, peroxo and oxo to the metal center indicating a strong ligand-to-metal charge transfer (LMCT) character.

The calculated high-energy bands at ca. 206.33, 202.63, and 205.25 nm for the complexes 1^- , 2^- , and 3^- are correlated with the experimentally obtained bands at ca. 204, 202, and 205 nm, respectively. These transitions mainly arise from high-energy ligand-to-ligand charge transfer (LLCT) transitions [20]. Thus, the theoretical simulated transitions are in close agreement with those observed experimentally.

Conclusion

The present work afforded water-soluble potassium(aquo) oxodiperoxo–tungstate(VI) complexes **1**, **2**, and **3** containing benzene-core carboxylic acids as the hetero-ligands. The chemical and spectral data obtained provided satisfactory evidence regarding composition of the coordination polyhedra and the likely mode of coordination of the ligands to WO^{4+} center. Density functional theory (DFT) computation studies on the complexes substantiated the experimental data. Reactivity of the oxoperoxo–tungstate(VI) complex, viz., compound **2**, was exploited to generate an active brominating species in situ to perform bromination of organic substrates efficiently.

Experimental

Chemicals used were reagent-grade products. The pH of the reaction solution was measured using a Systronics digital pH meter 335 and by BDH indicator paper. Molar conductance measurements were carried out in aqueous solution by Systronics conductivity meter-304. FT-IR spectra were recorded with KBr pellet on a PerkinElmer model spectrum 100 spectrometer. Electronic spectra were recorded (10^{-3} M aqueous solution) using Shimadzu

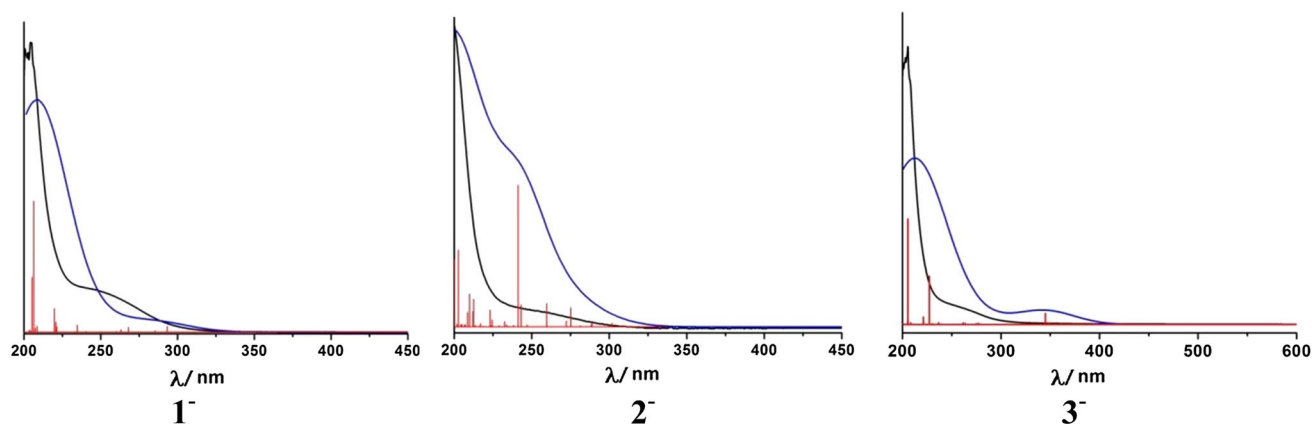


Fig. 3 The experimental (black), calculated (blue) electronic absorption spectra and the calculated electronic transitions (red) of 1^- , 2^- , and 3^- (color figure online)

Table 4 Electronic transitions of 1^- , 2^- , and 3^- calculated in water using the TD-DFT method

| Most important orbital excitations | λ | F | Experimental λ (ϵ) |
|--|-----------|---------|---------------------------------------|
| 1^- | | | |
| H \rightarrow L, H \rightarrow L+2 | 293.29 | 0.0120 | |
| H-1 \rightarrow L, H-1 \rightarrow L+2, H \rightarrow L+3 | 267.97 | 0.0098 | 245 (5708) |
| H-1 \rightarrow L+3, H-1 \rightarrow L+3, H-1 \rightarrow L+3 | 263.17 | 0.0054 | |
| H-2 \rightarrow L, H-2 \rightarrow L+1, H-2 \rightarrow L+4 | 234.70 | 0.0144 | |
| H-4 \rightarrow L+2, H-4 \rightarrow L+2 | 221.36 | 0.0108 | |
| H-2 \rightarrow L+4, H-2 \rightarrow L+4, H-3 \rightarrow L+1 | 220.70 | 0.0206 | |
| H-2 \rightarrow L+4, H-2 \rightarrow L+4, H-3 \rightarrow L+4, H-3 \rightarrow L+1 | 219.77 | 0.0485 | |
| H-4 \rightarrow L+4, H-5 \rightarrow L | 208.52 | 0.0121 | |
| H-4 \rightarrow L+4, H-5 \rightarrow L, H-4 \rightarrow L+4 | 207.33 | 0.0080 | |
| H-5 \rightarrow L+1, H-5 \rightarrow L+3, H-1 \rightarrow L+4 | 206.33 | 0.2681 | 204 (36,853) |
| H-6 \rightarrow L+2, H-5 \rightarrow L+2, H-6 \rightarrow L+2, H \rightarrow L+6 | 205.18 | 0.1123 | |
| H-6 \rightarrow L, H-6 \rightarrow L+1 | 203.44 | 0.0043 | |
| 2^- | | | |
| H \rightarrow L, H-1 \rightarrow L+1, H-2 \rightarrow L+1, H-2 \rightarrow L+3, | 288.89 | 0.0097 | |
| H-2 \rightarrow L, H-2 \rightarrow L+2, H-1 \rightarrow L+2 | 288.43 | 0.0056 | |
| H-1 \rightarrow L, H-3 \rightarrow L, H-2 \rightarrow L+2, H-3 \rightarrow L+4 | 275.23 | 0.0457 | |
| H-2 \rightarrow L, H-2 \rightarrow L+2, H-1 \rightarrow L, H-4 \rightarrow L | 272.34 | 0.0139 | |
| H-4 \rightarrow L, H-3 \rightarrow L, H-1 \rightarrow L+1 | 259.67 | 0.0560 | |
| H-3 \rightarrow L+1, H-4 \rightarrow L+1, H-3 \rightarrow L | 243.23 | 0.0526 | |
| H-1 \rightarrow L+2, H-4 \rightarrow L+1, H-3 \rightarrow L, H-3 \rightarrow L+1 | 241.26 | 0.3395 | 240sh (1520) |
| H-3 \rightarrow L+2, H-4 \rightarrow L+2 | 232.55 | 0.0127 | |
| H \rightarrow L+6, H-2 \rightarrow L+6, H-2 \rightarrow L+7, H-6 \rightarrow L+1, H-6 \rightarrow L+2, | 224.52 | 0.0165 | |
| H-6 \rightarrow L+1, H-5 \rightarrow L+1, H-2 \rightarrow L+6, H-7 \rightarrow L+1 | 223.13 | 0.0409 | |
| H-7 \rightarrow L+1, H-5 \rightarrow L+1, H-11 \rightarrow L+1, H-10 \rightarrow L+1 | 212.52 | 0.0665 | |
| H-6 \rightarrow L, H-6 \rightarrow L+3, H-5 \rightarrow L, H-6 \rightarrow L+1 | 212.12 | 0.0371 | |
| H-3 \rightarrow L+4, H-1 \rightarrow L+4, H-1 \rightarrow L+5, H-1 \rightarrow L+6 | 209.89 | 0.0790 | |
| H-7 \rightarrow L+3, H-6 \rightarrow L+3, H-6 \rightarrow L, H-7 \rightarrow L+1 | 208.60 | 0.0349 | |
| H-1 \rightarrow L+4, H-1 \rightarrow L+6, H-6 \rightarrow L+7, H-1 \rightarrow L+8 | 202.63 | 0.1843 | 202sh (4875) |
| 3^- | | | |
| H \rightarrow L, H \rightarrow L+1 | 348.68 | 0.01154 | |
| H-1 \rightarrow L, H \rightarrow L+1, H \rightarrow L+2 | 345.01 | 0.06748 | 250sh (2350) |
| H-3 \rightarrow L, H-3 \rightarrow L+3, H-2 \rightarrow L | 261.50 | 0.0110 | |
| H \rightarrow L+5, H-3 \rightarrow L+1, H-2 \rightarrow L, H-2 \rightarrow L+1 | 236.69 | 0.01195 | |
| H-2 \rightarrow L+1, H \rightarrow L+5, H-2 \rightarrow L, H-2 \rightarrow L+1 | 227.09 | 0.29123 | |
| H-3 \rightarrow L+2, H-2 \rightarrow L+2, H \rightarrow L+7 | 221.06 | 0.04589 | |
| H-5 \rightarrow L, H-4 \rightarrow L | 208.29 | 0.01127 | |
| H \rightarrow L+7, H-2 \rightarrow L+1, H-2 \rightarrow L+2 | 205.46 | 0.63378 | |
| H-1 \rightarrow L+6, H-3 \rightarrow L+4, H-2 \rightarrow L+3, H-2 \rightarrow L+4 | 205.25 | 0.01982 | 205 (33,537) |

λ wavelength (nm), ϵ molar absorption coefficient ($\text{dm}^3 \text{mol}^{-1} \text{cm}^{-1}$), f oscillator strength, H highest occupied molecular orbital, L lowest unoccupied molecular orbital

1800 spectrophotometer. The magnetic susceptibility was measured by Gouy method using $\text{HgCoN}_4\text{C}_4\text{S}_4$ as the calibrant. The ESI mass spectra were recorded on a Waters Qtof micro YA263 spectrometer in positive mode. TGA analysis was performed using PerkinElmer model Pyris 6 TGA 4000 at heating rate of $10^\circ\text{C}/\text{min}$ under atmosphere of nitrogen. ^1H NMR spectra with D_2O as solvent were

recorded using model Bruker AVANCE III HD Nanobay 400 MHz spectrometer. The products of bromination reactions were analyzed using GC-MS instrument model Varian 250-GC, Varian 240-MS using helium as the carrier gas ($1 \text{ cm}^3/\text{min}$) equipped with Varian capillary column ($30 \text{ m} \times 0.25 \text{ mm} \times 0.39 \text{ mm}$).

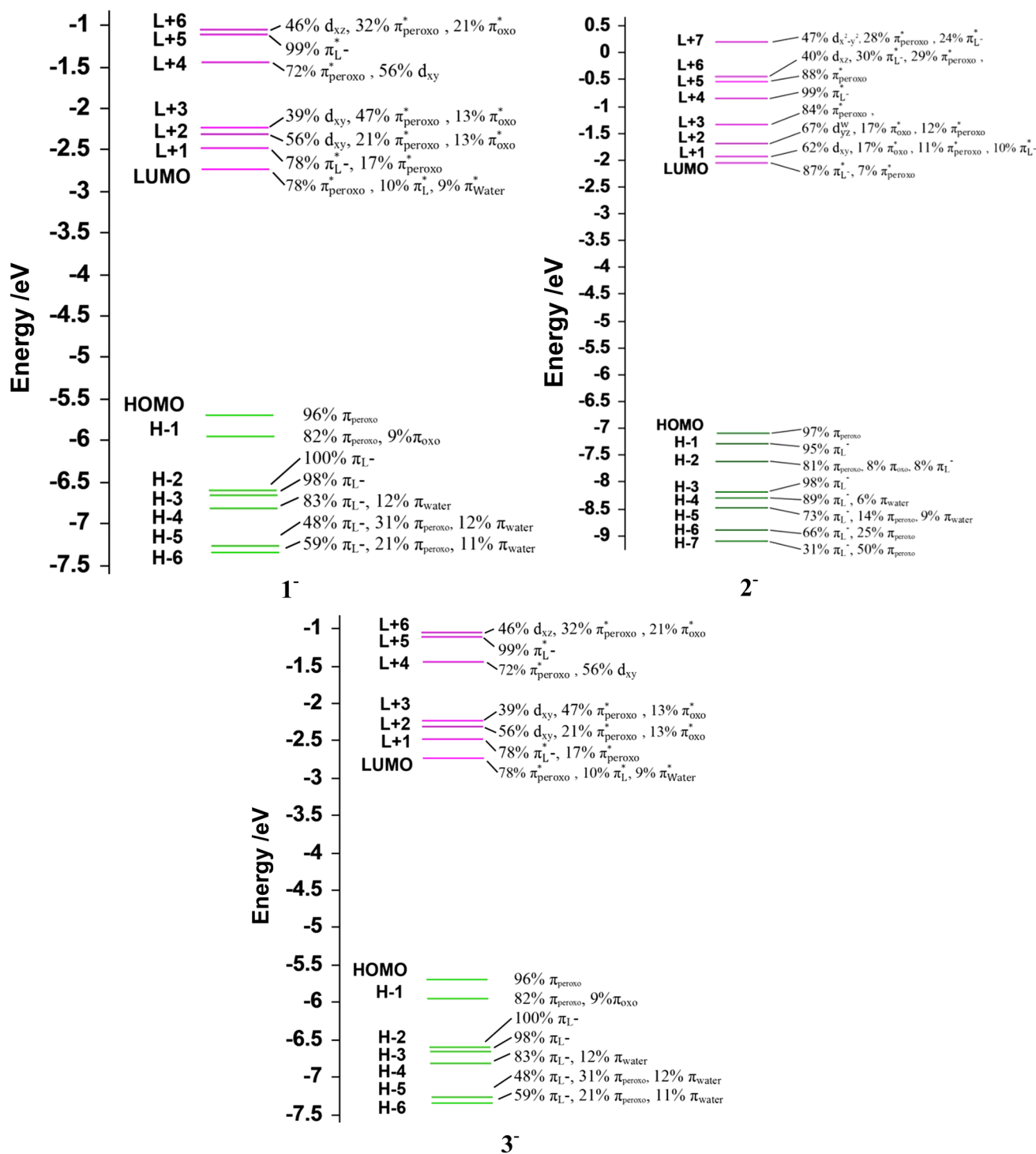


Fig. 4 The MO diagram of 1⁻, 2⁻, 3⁻ showing the character and energy (eV)

Elemental analyses

Tungsten was estimated gravimetrically as WO₄C₁₈H₁₂N₂ [56]. Peroxide contents were determined by redox titration with standard solutions of KMnO₄ and ceric ammonium

nitrate [57]. C, H, and N contents were determined by micro-analytical method.

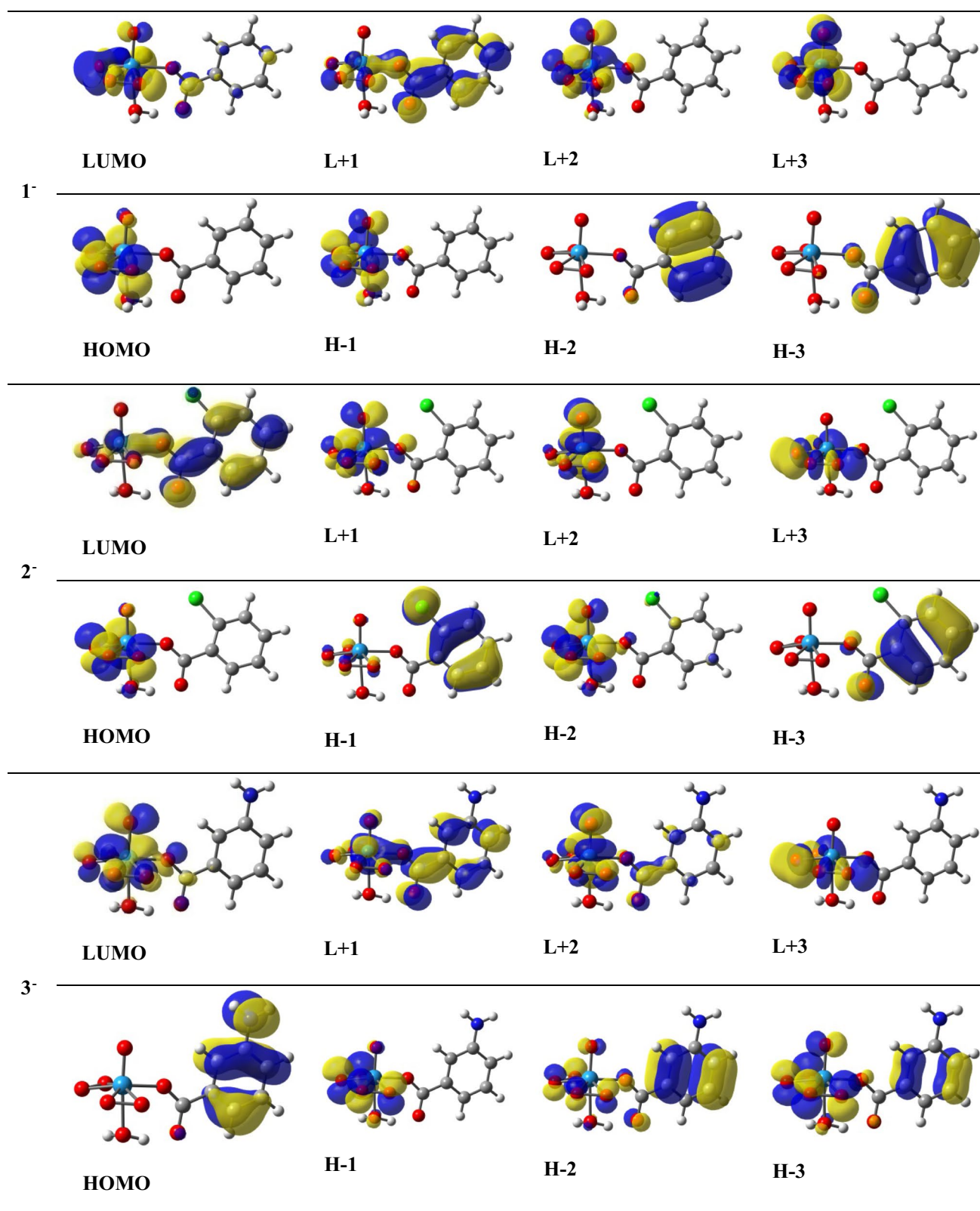


Fig. 5 Selected HOMOs and LUMOs of 1^- , 2^- , and 3^- . Positive values of the orbital contour are represented in yellow (0.03 au) and negative values in blue (-0.03 au) (color figure online)

Computational methods

The GAUSSIAN-09 Revision C.01 program package was used for all calculations [58]. The gas phase geometries of the molecular species (**1**[−], **2**[−], **3**[−]) were optimized fully unrestricting symmetry in singlet ground states with BPV86 functionals. The basis set LANL2DZ with effective core potential (ECP) was employed for W following the associated valence double ζ basis set of Hay and Wadt [59]. This is in combination with 6–31 + G** basis set selected for hydrogen, carbon, nitrogen, oxygen and chlorine [60, 61]. The same basis sets and functionals were used for calculation of vibrational frequencies. The electronic spectra of molecular ions (**1**[−], **2**[−], and **3**[−]) were calculated with the TD-DFT method, and the solvent effect (aqueous solution) was simulated using the polarizing continuum model with the integral equation formalism (C-PCM) [62, 63].

Synthesis of complexes (general procedure)

The method consists of dissolving 1 g Na₂WO₆H₄ (3.303 mmol) in 15 cm³ of water followed by gradual addition of 20 cm³ of 30% H₂O₂ (176.4 mmol) with continuous stirring, keeping the reaction temperature below 4 °C in an ice bath. To the resultant solution, benzoic acid or its derivative (3.303 mmol) dissolved in 10 cm³ ethanol was added in small portions and stirring continued for a period of 15 min, when reaction solution gradually changed from colorless to light yellow. The pH of the reaction mixture at that stage was found to be ca. 5–6. Potassium hydroxide solution (2 M) was added dropwise with constant stirring to raise the pH of the reaction medium to ca. 7–7.5. Addition of 50 cm³ pre-cooled acetone to the reaction mixture with stirring led to separation of white microcrystalline product. Product was allowed to settle, separated by centrifugation, washed with small volume of cold acetone and dried in vacuo over anhydrous CaCl₂. In solid state, the compounds were found to be stable in sealed polythene bags for prolong period at room temperature.

Potassium(aquo)(benzoato)oxodiperoxotungstate(VI)dihydrate (1, KWO₁₀C₇H₁₁) Yield 77.27%; IR (KBr): $\bar{\nu}$ = 3419 (O–H), 1640 (ν_{asy} CO₂[−]), 1431 (ν_{sym} CO₂[−]), 914 (ν W=O), 829 (ν O–O), 694 (ν_{asy} W–O₂), 565 (ν_{sym} W–O₂) cm^{−1}; UV–Vis (water): λ_{max} (ϵ) = 245 (5708) nm (mol^{−1} dm³ cm^{−1}); MS: m/z = 478.79, 426.13, 235.21.

Potassium(aquo)(2-chlorobenzoato)oxodiperoxotungstate(VI)dihydrate (2, KWO₁₀C₇H₁₀Cl) Yield 75.69%; IR (KBr): $\bar{\nu}$ = 3421 (ν O–H), 1640 (ν_{asy} CO₂[−]), 1459 (ν_{sym} CO₂[−]), 907 (ν W=O), 838 (ν O–O), 696 (ν_{asy} W–O₂), 547 (ν_{sym} W–O₂) cm^{−1}; UV–Vis (water): λ_{max} = 240sh (1520

nm (mol^{−1} dm³ cm^{−1}), MS: m/z = 494.76, 478.79, 394.85, 358.81.

Potassium(3-aminobenzoato)(aquo)oxodiperoxotungstate(VI)dihydrate (3, KWO₁₀C₇H₁₂N) Yield 74.32%; IR (KBr): $\bar{\nu}$ = 3502 br (ν O–H), 1606 (ν_{asy} CO₂[−]), 1434 (ν_{sym} CO₂[−]), 914 (ν W=O), 829 (ν O–O), 734 (ν_{asy} W–O₂), 565 (ν_{sym} W–O₂), 3424 (ν C–H); (ν N–H) cm^{−1}; UV–Vis (water): λ_{max} = 261.34 (2350) nm (mol^{−1} dm³ cm^{−1}); MS: m/z = 494.75, 478.78, 410.80.

Bromination of organic substrates and product analysis

In a representative procedure, organic substrates (1.0 mmol) were added to a solution of acetonitrile/water (1:1, 8 cm³) containing KBr (2 mmol). An accurately weighed amount of compound **2** (1.0 mmol) was added to the reaction mixture at room temperature with continuous stirring. Stirring was continued for a further period of ca. 4–5 h. The completion of the reaction was monitored by thin-layer chromatography (TLC). The reaction products as well as the unreacted organic substrates were separated by column chromatography. The reaction products were analyzed by GC–MS using benzophenone as internal standard.

Acknowledgements The authors are thankful to Tripura University for providing the infrastructure facilities; Prof. A. Saikia, Department of Chemistry, I.I.T Guwahati, for cooperation in recording of mass spectra. N. D is grateful to Tripura University for award of research fellowship (No. F.TU/REG/Ph.D/(Admn)/01/12) RET (UGC, New Delhi, India, sponsored). Authors are thankful to DST, Govt. of India, for providing 400 MHz NMR spectrometer to Tripura University under Fist program (SR/FST/CSI-263/2015). We are thankful to esteemed reviewers for helpful comments at the stage of revision.

References

1. Tsitsias V, Maniatakou A, Raptopoulou C, Karaliota A (2009) Polyhedron 28:3400
2. Butler A, Clague MJ, Meister GE (1994) Chem Rev 94:625
3. Mimoun M, Mignard P, Brechot P, Saussine L (1986) J Am Chem Soc 108:3711
4. Mizuno N, Yamaguchi K, Kamata K (2005) Coord Chem Rev 249:1944
5. Santos ICMS, Almeida Paz FA, Simoes MMQ, Neves MGPMS, Cavaleiro JAS, Klinowski J, Cavaleiro AMV (2008) Appl Catal A 351:166 (references therein)
6. Conte V, Floris B (2011) J Chem Soc Dalton Trans 73:1419 (references therein)
7. Gogoi SR, Boruah JJ, Sengupta G, Saikia G, Ahmed K, Bania KK, Islam NS (2015) Catal Sci Technol 5:595
8. Ma XT, Xing N, Yan ZD, Zhang XX, Wu Q, Xing YH (2015) New J Chem 39:1067
9. Kenneth S, Kirshenbaum KS, Sharpless KB (1985) J Org Chem 50:1979

10. Bortolini O, Furia FD, Modena G, Seragila R (1985) *J Org Chem* 50:2688
11. Dickman MH, Pope MT (1994) *Chem Rev* 94:569
12. Gresley NM, Griffith WP, Laemnael AC, Nogueira HIS, Parkin BC (1997) *J Mol Catal A* 117:185
13. Maiti SK, Banerjee S, Mukherjee AK, Malik KMA, Bhattacharya R (2005) *New J Chem* 29:554
14. Jimtaisong A, Luck RL (2006) *Inorg Chem* 45:10391
15. Le J, Elberg G, Gelfel D, Shechter Y (1995) *Biochemistry* 34:6218
16. Rao AVS, Islam NS, RamaSarma T (1997) *Arch Biochem Biophys* 342:289
17. Sels B, Devas D, Burtinx M, Pierard F, Jacobs P (1999) *Nature (London)* 400:855
18. Bora U, Choudhury MK, Dey D, Dhar SS (2001) *Pure Appl Chem* 73:93
19. Burke A (2008) *J Coord Chem Rev* 252:170
20. Das N, Chowdhury S, Dutta Purkayastha RN (2017) *J Chin Chem Soc* 64:43
21. Clague MJ, Butler A (1995) *J Am Chem Soc* 117:3475
22. Badetti E, Romano F, Marchio L, Taskesenlioglu S, Dastan A, Zonta C, Licini G (2016) *Dalton Trans* 45:14603 (references therein)
23. Sels BF, Devis DE, Jacobs PA (2003) *J Catal* 216:288
24. Maurya MR, Kumar U, Manikandan P (2006) *Dalton Trans* 29:3561
25. Butler A, Walker JV (1993) *Chem Rev* 93:1937
26. Clark JH, Ross JC, Macquarrie DJ, Barlow SJ, Bastock TW (1997) *Chem Commun* 13:1203
27. Bhattacharjee M, Choudhury MK, Dutta Purkayastha RN (1986) *Inorg Chem* 25:2354
28. Tamami B, Yeganeh H (1999) *Eur Polym J* 35:1445
29. Kalita D, Sarmah S, Das SP, Baishya D, Patowary A, Baruah S, Islam NS (2008) *React Funct Polym* 68:876
30. Gabriel C, Kaliva M, Vanetis J, Baran P, Rodriguez-Escudero I, Voyiatzis G, Zervou M, Salifoglou A (2009) *Inorg Chem* 48:476
31. Bora U, Bose G, Choudhury MK, Dhar SS, Gopinath R, Khan AT, Patel BK (2000) *Org Lett* 2:247
32. Landaeta VR, Rodriguez-Lugo RE (2015) *Inorg Chim Acta* 431:21
33. Dengel AC, Griffith WP, Powell RD, Skapski AC (1987) *J Chem Soc Dalton Trans*. <https://doi.org/10.1039/DT9870000991>
34. Djordjevic C (1982) *Chem Br* 18:554
35. Campbell NJ, Dengal AC, Griffith WP (1989) *Polyhedron* 8:1379
36. Griffith WP (1963) *J Chem Soc* 5345
37. Griffith WP (1964) *J Chem Soc* 5248
38. Gubelmann MH, Williams AF (1983) *Structure and bonding*. Springer-Verlag, Berlin, Heidelberg
39. Nakamoto K (2008) *Infrared and Raman Spectra of Inorganic and coordination compounds*, 6th edn. Wiley Interscience, London
40. Deacon GB, Philips RJ (1980) *Coord Chem Rev* 33:227
41. Yang CT, Vetrichelvan M, Yang X, Moubakari B, Murray KS, Vital JJ (2004) *J Chem Soc Dalton Trans* 113
42. Connor JA, Ebsworth EAV (1964) *Adv Inorg Chem Radio Chem* 6:279
43. Nath M, Yadav R, Eng G, Musingarimi P (1999) *Appl Organomet Chem* 13:29
44. Girasolo MA, Rubino S, Portanova P, Calvaruso G, Ruisi G, Stocco G (2010) *J Organomet Chem* 695:609
45. Valentin CD, Gisdakis P, Yudanov IV, Rösch N (2000) *J Org Chem* 65:2996
46. Maiti SK, Malik KMA, Bhattacharyya R (2004) *Inorg Chem Commun* 7:823
47. Badetti E, Romano F, Marchiò L, Taşkesenlioglu S, Daştan A, Zonta C, Licini G (2016) *Dalton Trans* 45:14603
48. Sergienko VS (2008) *Crystallogr Rep* 53:22
49. Kamata K, Kuzuya S, Uehara K, Yamaguchi S, Mizuno N (2007) *Inorg Chem* 46:3768
50. Santos ICMS, Paz FAA, Simões MMQ, Neves MGPM, Cavaleiro JAS, Klinowski J, Cavaleiro AMV (2008) *Appl Catal A: Gen* 351:166
51. Sundaraganesan N, Joshua BD, Radjakoumar T (2009) *Indian J Pure Appl Phys* 47:248
52. Westland AD, Haque F, Bouchard JM (1980) *Inorg Chem* 19:2255
53. Campbell NJ, Dengel AC, Edwards CJ, Griffith WP (1989) *J Chem Soc Dalton Trans* 1989:1203
54. Saha P, Naskar J, Bhattacharya A, Ganguly R, Saha B, Chowdhury S (2016) *J Coord Chem* 69:303
55. Sharma M, Sheikh HN, Pathania MS, Kalsotra BL (2008) *J Coord Chem* 61:426
56. Vogel AI (1962) *Textbook of quantitative inorganic analysis*. Longmans, Green, London, p 566
57. Vogel AI (1962) *Textbook of Quantitative Inorganic Analysis*. Longmans, Green, London, p 295, 325
58. Frisch MJ, Trucks GW, Schlegel HB, Scuseria GE, Robb MA, Cheeseman JR, Scalmani G, Barone V, Mennucci B, Petersson GA, Nakatsuji H, Caricato M, Li X, Hratchian HP, Izmaylov AF, Bloino J, Zheng G, Sonnenberg JL, Hada M, Ehara M, Toyota K, Fukuda R, Hasegawa J, Ishida M, Nakajima T, Honda Y, Kitao O, Nakai H, Vreven T, Montgomery JA Jr, Peralta JE, Ogliaro F, Bearpark M, Heyd JJ, Brothers E, Kudin KN, Staroverov VN, Kobayashi R, Normand J, Raghavachari K, Rendell A, Burant JC, Iyengar SS, Tomasi J, Cossi M, Rega N, Millam JM, Klene M, Knox JE, Cross JB, Bakken V, Adamo C, Jaramillo J, Gomperts R, Stratmann RE, Yazyev O, Austin AJ, Cammi R, Pomelli C, Ochterski JW, Martin RL, Morokuma K, Zakrzewski VG, Voth GA, Salvador P, Dannenberg JJ, Dapprich S, Daniels AD, Farkas Ö, Foresman JB, Ortiz JV, Cioslowski J, Fox DJ (2009) *Gaussian 09*, Revision C.01. Gaussian Inc, Wallingford, CT
59. Hay PJ, Wadt WR (1985) *J Chem Phys* 82:299
60. Hehre WJ, Ditchfield R, Pople JA (1972) *J Chem Phys* 56:2257
61. Dill JD, Pople JA (1975) *J Chem Phys* 62:2921
62. Barone V, Cossi M (1998) *J Phys Chem A* 102:1995
63. Tomasi J, Mennucci B, Cammi R (2005) *Chem Rev* 105:2999

Publisher's Note Springer Nature remains neutral with regard to jurisdictional claims in published maps and institutional affiliations.